Experimental super-Heisenberg quantum metrology with indefinite gate order

Peng Yin
University of Science and Technology of China
Xiaobin Zhao
The University of Hong Kong
Yuxiang Yang
The University of Hong Kong
Yu Guo
USTC https://orcid.org/0000-0002-1962-7343
Wen-Hao Zhang
University of Science and Technology of China
Gong-Chu Li
University of Science and Technology of China
Yong-Jian Han
University of Science and Technology of China
Bi-Heng Liu
CAS Key Laboratory of Quantum Information, University of Science and Technology of China, Hefei, 230026, People's Republic of China https://orcid.org/0000-0002-4569-7716
Jin-Shi Xu
University of Science and Technology of China https://orcid.org/0000-0003-0528-1000
Giulio Chiribella
The University of Hong Kong
Geng Chen
University of Science and Technology of China
Chuan-Feng Li (cfli@ustc.edu.cn)
University of Science and Technology of China https://orcid.org/0000-0001-6815-8929
Guangcan Guo
University of Science and Technology of China

Article

Keywords:

Posted Date: February 23rd, 2022

DOI: https://doi.org/10.21203/rs.3.rs-1327792/v1

Experimental super-Heisenberg quantum metrology with indefinite gate order

Peng Yin,[1,2,*] Xiaobin Zhao,[3,*] Yuxiang Yang,[3,4] Yu Guo,[1,2] Wen-Hao Zhang,[1,2] Gong-Chu Li,[1,2] Yong-Jian Han,[1,2] Bi-Heng Liu,[1,2] Jin-Shi Xu,[1,2] Giulio Chiribella,[3,5,6,†] Geng Chen,[1,2,‡] Chuan-Feng Li,[1,2,§] and Guang-Can Guo[1,2]

[1]*CAS Key Laboratory of Quantum Information, University of Science and Technology of China, Hefei 230026, People's Republic of China*

[2]*CAS Center For Excellence in Quantum Information and Quantum Physics, University of Science and Technology of China, Hefei, Anhui 230026, China*

[3]*QICI Quantum Information and Computation Initiative, Department of Computer Science, The University of Hong Kong, Pokfulam Road, Hong Kong 999077, China*

[4]*Institute for Theoretical Physics, ETH Zürich, 8093 Zürich, Switzerland*

[5]*Department of Computer Science, University of Oxford, Parks Road, Oxford OX1 3QD, United Kingdom*

[6]*Perimeter Institute for Theoretical Physics, Caroline Street, Waterloo, Ontario N2L 2Y5, Canada*

(Dated: February 4, 2022)

Abstract

The Heisenberg limit, corresponding to a root mean square error vanishing as $1/N$ with the number N of independent processes probed in an experiment, is widely believed to be an ultimate limit to the precision of quantum metrology. In this work, we experimentally demonstrate a quantum metrology protocol surpassing Heisenberg limit by implementing indefinite (a superposition of) orders of two groups of independent processes. Each process creates a phase space displacement, and the precision to estimate the geometric phase introduced by a total number of $2N$ processes approaches the super-Heisenberg limit $1/N^2$. In our setup, the polarization of a single photon coherently controls the order of displacements on the transverse modes of the radiation field, resulting into indefinite order and allowing us to outperform every setup where the displacements are probed in a definite order. Our experiment features a realization of coherent control over the order in a continuous-variable system, and can be applied to the measurement of various important parameters.

INTRODUCTION

Quantum metrology [1–3] is one of the most promising near-term quantum technologies. Its core promise is that quantum resources, such as entanglement and coherence, can improve the precision of measurements beyond the limits of classical setups. The paradigmatic example is the reduction of the root mean square error (RMSE) from the standard quantum limit (SQL) $1/\sqrt{N}$ to the Heisenberg limit $1/N$ for the estimation of a parameter from N independent processes, or from N independent applications of the same process. The Heisenberg scaling has been demonstrated in a variety of setups, e.g., by preparing N entangled probes [4–6], or by letting a single probe evolve sequentially through the N processes under consideration [7, 8]. Generally, the Heisenberg limit $1/N$ is regarded as the ultimate quantum limit for independent processes [9]. Scalings beyond the Heisenberg limit are known in the presence of inefficient detectors [10], nonlinear interactions among N particles [11–15], or non-Markovian correlations between N processes [16]. However, such enhancements typically do not apply to the basic scenario of N independent processes.

Recently, research in the foundations of quantum mechanics identified a new quantum resource that could be exploited in quantum metrology, potentially breaking the $1/N$ barrier of the Heisenberg limit [17]. Such resource is the ability to combine quantum processes in a superposition of alternative orders, using a primitive known as the quantum SWITCH [18, 19]. The quantum SWITCH is a hypothetical machine that operates on physical processes, taking two processes as input and letting them act in an order controlled by the state of a quantum particle. Originally motivated by foundational questions about causality in quantum mechanics [20, 21], the research on the applications of the quantum SWITCH has revealed a number of information-processing advantages in various tasks, including quantum channel discrimination [22, 23], distributed computation [24], quantum communication [25] and quantum thermodynamics [26]. The application to quantum metrology was recently explored in a series of theoretical works [17, 27–29]. In particular, Ref. [17] identified a scenario where the ability to coherently control the order of $2N$ independent processes on an infinite dimensional system enables the estimation of a geometric phase with a super-Heisenberg scaling $1/N^2$. This enhancement was shown to be due to the indefinite order in which the unknown processes are probed: any setup that probes the same $2N$ processes in a definite order using a finite amount of energy will necessarily be subject to the Heisenberg

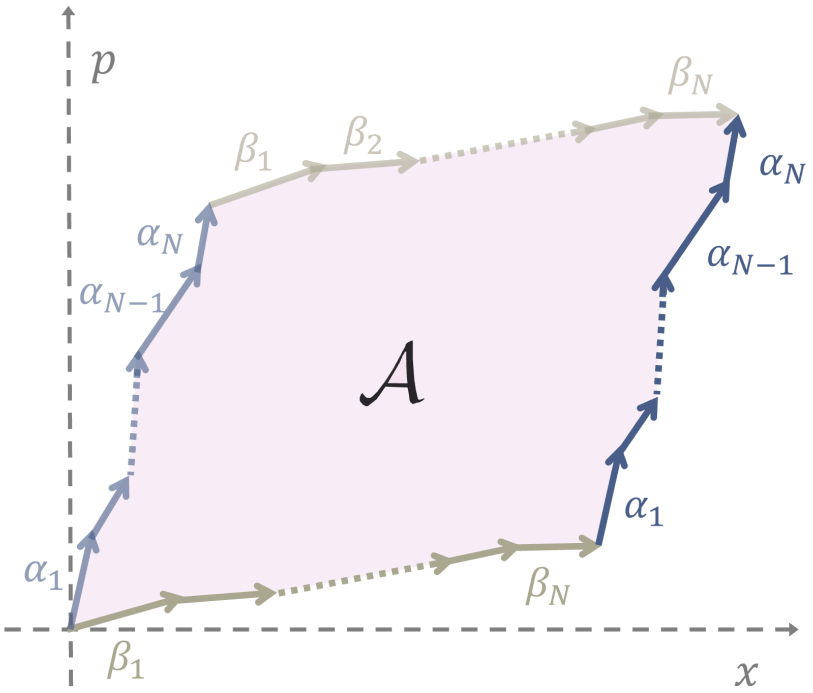

FIG. 1: **Geometric phase associated to two sets of phase space displacements.** The displacements take place in the plane associated to two canonically conjugated variables x and p. The first set consists of displacements $\{\alpha_1, \ldots, \alpha_N\}$ (in blue), while the second consists of displacements $\{\beta_1, \ldots, \beta_N\}$ (in grey). When the two sets of displacements are performed in two alternative orders, they give rise to two paths that enclose an area $\mathcal{A}$, corresponding to the geometric phase associated to a continuous variable quantum system subject to two sequences of phase space displacements in two alternative orders.

scaling $1/N$.

While the theory indicates that the ability to coherently control the order is a resource for quantum metrology, the benefits of this resource had not been observed experimentally until now. For the demonstration of the super-Heisenberg scaling metrological protocol, the main challenge is that the setup of Ref. [17] requires coherent control over the order of operations in an infinite dimensional, continuous variable system, which is beyond the state of the art of the existing experiments [30–36].

Here, we initiate the application of indefnite gate order in quantum metrology, by building a photonic quantum Switch in a continuous-variable system. The setup is used to estimate

the geometric phase associated to two groups of N phase space displacements, as illustrated in Fig. 1. By combining the two groups of displacements in a coherent superposition of orders, we experimentally observe an $1/N^2$ scaling of error, which beats the scaling achievable by every setup where the probed processes are arranged in a definite gate order. Our proof-of-principle demonstration opens up the exploration of new schemes for quantum metrology boosted by coherent control over the order.

RESULTS

Our experiment is conducted on a single-photon quantum system, with a discrete variable degree of freedom corresponding to the photon's polarization, and a continuous variable degree of freedom associated to the photon's transverse spatial modes. We consider a scenario where the continuous variable degree of freedom undergoes two sets of phase space displacements, with set S_1 consisting of displacements $\{D_{\alpha_j}\}_{j=1}^N$ and set S_2 consisting of displacements $\{D_{\beta_k}\}_{k=1}^N$, where $\{\alpha_j\}$ and $\{\beta_k\}$ are arbitrary complex numbers, regarded as shifts in two conjugate variables x and p, as shown in Fig. 1. The displacements in S_1 and S_2 determine two alternative paths in phase space: one path is generated by applying first the displacements in S_1 and then those in S_2, while the other path is generated by applying first the displacements in S_2 and then those in S_1. Together, the two paths identify a cycle encircling an area $\mathcal{A}$. The associated phase factor $e^{i\mathcal{A}}$ is an example of the geometric phase, in this case associated to the geometry of the plane.

We now provide an experimental setup for measuring the geometric phase approaching super-Heisenberg limit precision. Specifically, our setup provides an estimate of the regularized area $A := \mathcal{A}/N^2$, which is equal to the product of the average displacements $\overline{\alpha} = \sum_j \alpha_j/N$ and $\overline{\beta} = \sum_k \beta_k/N$. For simplicity, we will restrict our analysis to the case where set S_1 consists of position displacements $D_{x_j} := e^{-ix_jP}$, while set S_2 consists of momentum displacements $D_{p_k} := e^{ip_kX}$, with $X = (a + a^\dagger)/\sqrt{2}$ and $P = -i(a - a^\dagger)/\sqrt{2}$. Then, the task is to estimate $A = \bar{x}\bar{p}$, where $\overline{x}$ and $\overline{p}$ are the average x-displacement and the average p-displacement.

In the experiment, the x and p displacements are introduced by sets of customized birefringent MgF_2 plates and wedge pairs shown in Fig. 2 (see Methods). The x (p) displacements take slightly different values with fluctuations no more than $\pm 5\%$ around a reference value.

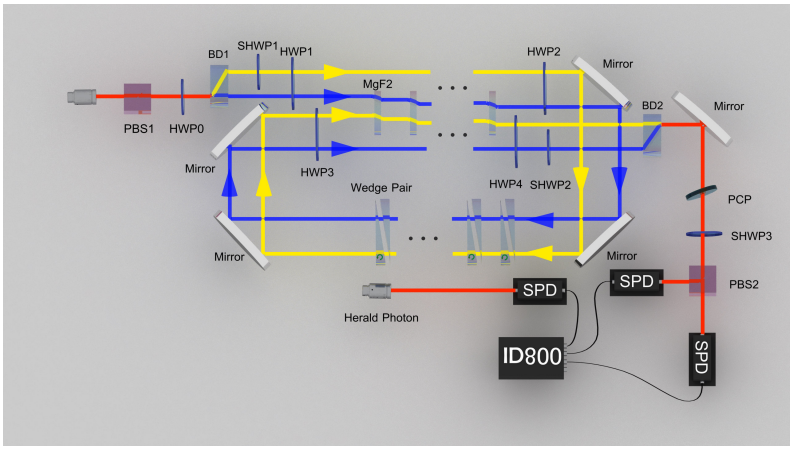

FIG. 2: **Experimental setup for coherently controlling gate orders in a continuous variable photonic system.** The experimental setup consists of three parts: (1) a polarization controller of heralded signal photons, (2) a Mach-Zehnder (M-Z) interferometer that provides control on the order, and (3) a polarization analyser (PA) to perform projective measurements on the control qubit. The signal and idler photon pairs are generated through a spontaneous parametric down conversion process by pumping Beta Barium Borate crystal (not shown in the figure) with $390nm$ light, and the signal photons are initialized to $\frac{1}{\sqrt{2}}(|H\rangle + |V\rangle)$ ($|H\rangle$ and $|V\rangle$ denote horizontal and vertical polarization) by PBS1 and HWP0. This coherent superposition in polarization is transformed into the coherent superposition between the two arms (denoted as yellow and blue arms) of the M-Z interferometer, which is composed of beam displacers (BD1 and BD2) and the optical components in between. The x and p displacements are caused by the MgF_2 plates and the wedge pairs, respectively. The two arms constitute the control qubit and the transmission of a single photon in a superposition of the two arms induces a a coherent superposition of two alternative orders of displacements on the transverse modes. At the end of the M-Z interferometer, the two arms are recombined by BD2 and transformed to a polarization qubit, which is projected to $|\pm\rangle := \frac{1}{\sqrt{2}}(|H\rangle \pm |V\rangle)$ by the PA (consisting of SHWP3 and PBS2). The two exits of PBS are connected to two single photon detectors (SPDs), and the corresponding clicks coincident with those generated by the idler photons are recorded by ID800.

For the x displacements, we have $x_j \approx 18.6\ \mu m$ for horizontally polarized ($|H\rangle$) photons. For the p displacements, we have $p_j \approx 2\pi\theta_j^{\text{eff}}/\lambda$ [37], where $\theta_j^{\text{eff}} \approx 2.8 \times 10^{-4}$ rad is the deflection angle associated to the wedge pair.

As shown in Fig. 2, The order of the displacements is controlled by the polarization

of a single photon, which is initialized in the state $(|H\rangle + |V\rangle)/\sqrt{2}$, where $|H\rangle$ and $|V\rangle$ denote the states of horizontal and vertical polarization. The preparation of control qubit is achieved by a polarization controller for heralded single photons, implemented by a polarizing beam splitter (PBS1) and a half-wave plate (HWP0). The superposition of polarizations then induces a superposition of paths through a M-Z interferometer, with the two paths traversing the two groups of displacements in opposite orders. Finally, at the output of the interferometer, the photon polarization is measured in the basis $\{|+\rangle, |-\rangle\}$, with $|\pm\rangle = (|H\rangle \pm |V\rangle)/\sqrt{2}$. Then a polarization analyser (PA) consisting of a phase compensation plate (PCP), a small half-wave plate (SHWP3) and a polarizing beam splitter (PBS2) is used to implement projective measurement on the polarization degree of freedom. When more x and p displacements are implemented, the required number of optical elements increases and a stochastic phase shift occurs. This stochastic phase messes up the estimated geometric phase and has to be eliminated before the running of quantum SWITCH (see the Methods for more details).

Our setup generates a coherent superposition of different orders of continuous-variable gates. Precisely, the setup reproduces the overall action of the quantum SWITCH, making the photon experience the x and p displacements in a coherent superposition of two alternative orders. The state of the photon right before the measurement is the superposition $\frac{1}{\sqrt{2}}\left(|H\rangle \otimes D_{p_N} \dots D_{p_1} D_{x_N} \dots D_{x_1}|\psi\rangle + e^{i\phi_0}|V\rangle \otimes D_{x_N} \dots D_{x_1} D_{p_N} \dots D_{p_1}|\psi\rangle\right)$, where $|\psi\rangle$ is the state of the transverse modes of a Gaussian beam and is set to the ground state of a harmonic oscillator. ϕ_0 is a constant offset for varying N, which is caused by the unevenness of the four full-sized HWPs (HWP1, HWP2, HWP3, and HWP4) (see Methods for more details).

When the photon's polarization is measured in the basis $\{|+\rangle, |-\rangle\}$, the probabilities of the possible outcomes are

$$P_{\pm} = \frac{1}{2}\left(1 \pm \cos(N^2 A + \phi_0)\right) . \tag{1}$$

Crucially, the phase exhibits a quadratic dependence on the number of displacements, leading to a super-Heisenberg sensitivity to small changes of A. In the experiment, we estimated the probability P_- for $N = 0, 1, 2, \cdots, 8$, as shown in Fig. 3. The data is in agreement with Eq. (1) with parameters $A = 0.042$ rad and $\phi_0 = 0.307$ rad.

The statistics is obtained by repeating the experiment for ν times. From the ob-

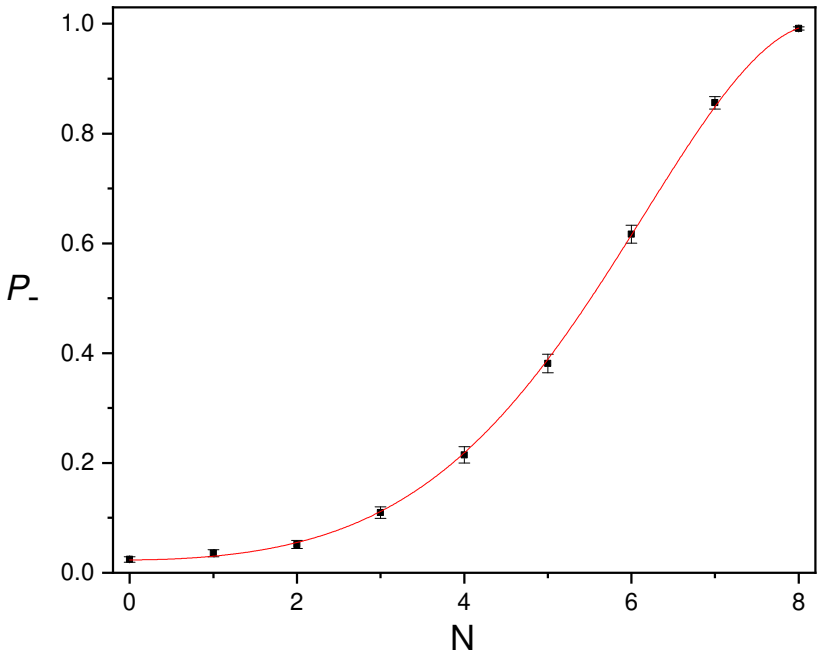

FIG. 3: P_- **for Varying** N**.** The black dots are the experimentally measured data of P_- for varying N. The red lines is the fitting of these dots with fitting function $\frac{1}{2}(1-\cos(N^2A+\phi_0))$. As we can see, all the data points falls at the fitting curve within the error-bar.

tained data, the phase A is then estimated with a maximum likelihood estimate $\hat{A} := \arg\max_A \log p(m_1,\ldots,m_\nu|A)$, where $m_j \in \{+,-\}$ is the j-th measurement outcome, and $p(m_1,\ldots,m_\nu|A)$ is the probability of obtaining the measurement outcomes $\{m_1,\ldots,m_\nu\}$ conditioned on the parameter being A. Theoretically, the RMSE of this parameter is [17]

$$\delta A = \frac{1}{\sqrt{\nu}N^2}. \tag{2}$$

The x (p) displacement can also be estimated through A if p (x) displacement is known, and the RMSE vanishes with same scaling of Eq. (2).

To indicate that indefinite causal order can boost the precision of quantum metrology, we use $\nu = 1000$ counts to calculate P_- in each trial of measurement, and the precision is defined as the RMSE of the results from 30 trials of measurement. The RMSE for different N are plotted in Fig. 4, and it is shown that δA decreases with super-Heisenberg scaling $\delta A \propto \frac{1}{N^2}$, as predicted by Ref. [17]. Furthermore, the quadratically fitted line (color black) approaches

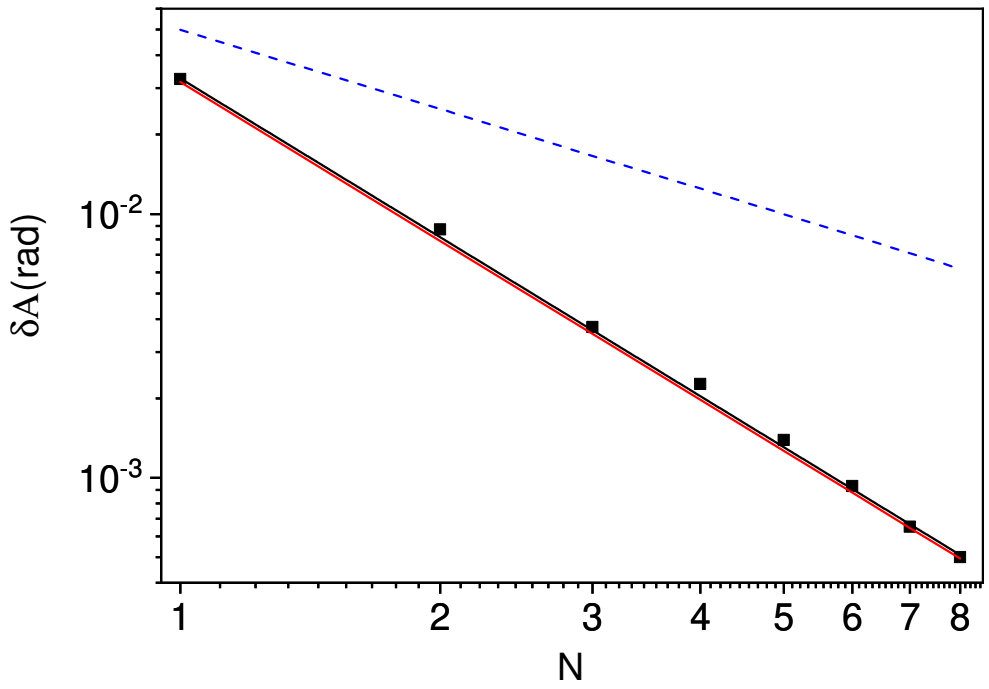

FIG. 4: **Super-Heisenberg scaling of the RMSE of** A. The black data points are the experimentally measured RMSE of A for varying N. The black line is the fitting of the data with fitting function $\frac{1}{cN^2}$ where $c \approx 30.65$ is the parameter for fitting. The red line represents the theoretical super-Heisenberg limit $\delta A = \frac{1}{\sqrt{\nu}N^2}$ with $\nu = 1000$. The dashed blue line is the theoretical lower bound on the RMSE for an experimentally feasible strategy with fixed order, analyzed in Supplementary Information.

the theoretical super-Heisenberg limit $\delta A = 1/(\sqrt{\nu}N^2)$ (color red). The super-Heisenberg limit approached in the experiment is in stark contrast with the ultimate limit achievable by probing the displacements in a fixed order, using probes with the same amount of energy as used in our experiment: as shown in Ref. [17] every setup with fixed order and minimum probe energy will necessarily lead to an RMSE with Heisenberg limited scaling $\propto 1/N$. In Fig. 4, we also compare the precision achieved in our experiment with the precision of an alternative, experimentally feasible strategy that achieves Heisenberg scaling by probing the displacements in a fixed order.

To further investigate the origin of the super-Heisenberg scaling in our experiment, we implemented another experimental test by keeping only one fixed p displacement while

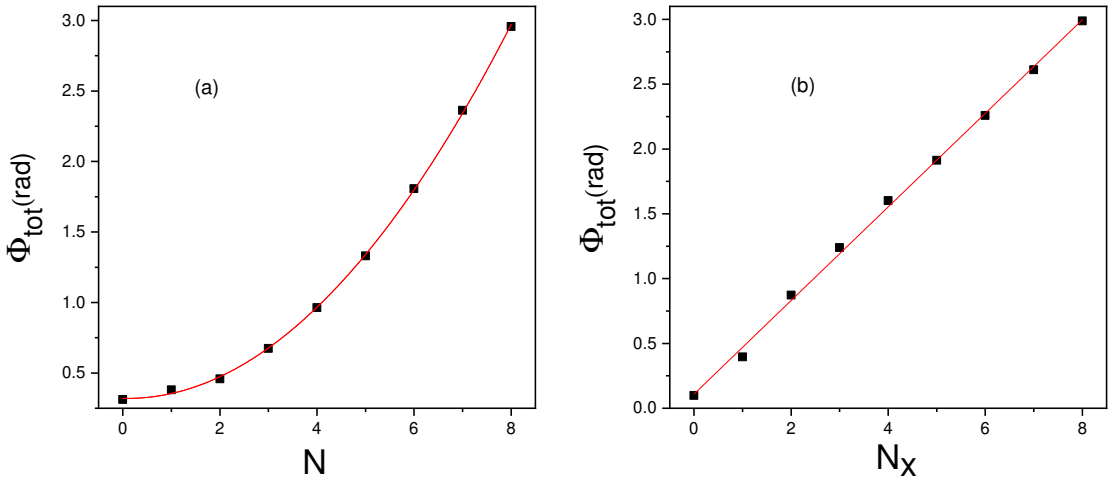

FIG. 5: **The scaling of the total phase against N.** (a) Total phase $\Phi_{\text{tot}} = N^2 A + \phi_0$ derived from Fig. 3. The black squares are the experimental data and the red line is the quadratic fitting. (b) Total phase Φ_{tot} for varying number of x-displacements when only one p-displacement is applied. The black squares are the experimental data and the red line is the linear fitting.

merely varying the number of x displacements. To be specific, we insert only one wedge pair into the setup and keep $\theta^{\text{eff}}_{single}$ fixed, and then we change the number of MgF_2 plates N_x from 0 to 8. The corresponding total phase is linear in N_x, as shown in Fig. 5 (b); by contrast, as shown in Fig. 5 (a), the total phase obtained with the original indefinite gate order protocol is quadratic in N, which yields a RMSE approaching super-Heisenberg limit. From this point of view, solely increasing the x (p) displacements cannot constitute the effective resources of an indefinite gate order protocol, and the resulted RMSE is Heisenberg-limited.

DISCUSSION

In this paper, we experimentally demonstrated the potential of coherent control over the order in quantum metrology. We built a photonic setup that estimates a geometric phase by combining two sets of displacements on the transverse spatial degrees of freedom of a single photon. Our setup achieves a precision approaching super-Heisenberg limit, which is impossible to achieve with any scheme that probes the same processes in a fixed order using the same amount of energy as our scheme. Our setup could be used to perform precision tests of the canonical commutation relations, and to detect tiny deviations from the standard

quantum values, such as those envisaged in certain theories of quantum gravity [38–41].

Besides the applications of our setup, it is interesting to explore further applications of the superposition of orders in quantum metrology. Theoretically, an interesting open question is whether is it possible to achieve super-Heisenberg scaling for discrete-variable systems like qubit, which is the basic building block of quantum information processing. Furthermore, it is interesting to explore whether the quadratic scaling $1/N^2$ is the ultimate limit achievable with indefinite gate order, or whether even more favourable scalings could be achieved with more complex architectures beyond the quantum SWITCH.

METHODS

Implementation of x and p displacements. As shown in Fig. 2, the x displacement is generated by the birefringence of a $2mm$-thick MgF_2 plate whose optical axis is at a 45° angle with x-axis in the x-z plane (the z-axis is defined as the propagating direction of photons and x-axis is defined as the direction of horizontal polarization). This configuration results into a reference displacement of approximately 18.6 μm along the x-axis when the photon is horizontally polarized ($|H\rangle$). The p displacement corresponds to a linear phase modulation of the photon along the x-direction, and is thus equivalent to a small deflection angle in the x-z plane (under the paraxial approximation). It is realized by a pair of wedges with the same wedge angle of 1°. Here the usage of the wedge pair enables a precise control of the p displacement by mechanically rotating the stages on which the wedges are mounted. By rotating one of the two wedges, we introduce a deflection angle $\theta^{\text{eff}} \approx 2.8 \times 10^{-4}$ rad(0.016°) of the photon, which in turn induces a linear phase modulation e^{ipX} with $p \approx 2\pi\theta^{\text{eff}}/\lambda$. For both x and p displacements, the exact values are not uniform across the N devices, and the fluctuation is no more than ±5% around the reference value.

Initialization of the optical setting. To demonstrate the advantage of coherent control on the order, an initialization of the M-Z interferometer is performed before the execution of quantum SWITCH. Here, the coherence of the control qubit is transformed back and forth between the path degree of freedom (yellow and blue arms in Fig. 2) and polarization degree of freedom (horizontal and vertical polarization). The main purpose of the initialization is to eliminate the initial phase between the two arms (denoted as yellow and blue) of the M-Z interferometer in Fig. 2, as such phase changes stochastically with the

number of optical elements inside the M-Z interferometer. In the initialization process, we firstly prepare the single photons into $|+\rangle := \frac{1}{\sqrt{2}}(|H\rangle + |V\rangle)$ by orienting HWP0 to 22.5°, and then we use BD1 to coherently split $|H\rangle$ and $|V\rangle$ components into two arms of the M-Z interferometer (denoted by yellow and blue lines), which serves as the control qubit. With the two small HWPs (SHWP1 and SHWP2) orienting at 45° , and the four full-sized HWPs (HWP1, HWP2, HWP3, and HWP4) oriented at 0°, the photons on the two arms are both $|V\rangle$ when passing the MgF_2 plates and no x displacement occurs thereby. With these settings, the two arms are recombined by BD2 without creating a geometric phase. By tilting the PCP, we can achieve a vanishing projection probability to $|-\rangle = \frac{1}{\sqrt{2}}(|H\rangle - |V\rangle)$ at the PA, the initial phase difference between the two arms is thus eliminated by the PCP. For a given N, to create a geometric phase, we only need to orient the four full-sized HWPs (HWP1, HWP2, HWP3, and HWP4) to 45°; and thus, the polarization of the photon is the same as that in the initialization step for all the elements in the setup except MgF_2 plates. To be specific, HWP1 and HWP3 tune the polarization of photons from $|V\rangle$ to $|H\rangle$, which implements the x displacement due to the birefringence of MgF_2 plates, HWP2 and HWP4 keep the polarization of photons unchanged for all other optical elements except the MgF_2 plates. From Fig. 2, we can see that the photon first experiences the p displacements and then the x displacements for the yellow arm, while it experiences the opposite order for the blue arm. Thanks to this mechanism, the polarization coherently controls the order of the x and p displacements, resulting in a superposition of alternative orders whenever the photon is prepared in a superposition of the $|H\rangle$ and $|V\rangle$ states. To probe the scaling of the precision of the geometric phase with the number of displacements, the above procedure (initialization and generation of the geometric phase) is repeated for different values of N.

---

* These authors contributed equally to this work

† Electronic address: giulio@cs.hku.hk

‡ Electronic address: chengeng@ustc.edu.cn

§ Electronic address: cfli@ustc.edu.cn

[1] Giovannetti, V., Lloyd, S. & Maccone, L. Quantum-enhanced measurements: beating the standard quantum limit. Science **306**, 1330–1336 (2004).

[2] Giovannetti, V., Lloyd, S. & Maccone, L. Quantum metrology. Physical Review Letters **96**, 010401 (2006).

[3] Giovannetti, V., Lloyd, S. & Maccone, L. Advances in quantum metrology. Nature photonics **5**, 222–229 (2011).

[4] Bollinger, J. J., Itano, W. M., Wineland, D. J. & Heinzen, D. J. Optimal frequency measurements with maximally correlated states. Physical Review A **54**, R4649 (1996).

[5] Walther, P. et al. De broglie wavelength of a non-local four-photon state. Nature **429**, 158–161 (2004).

[6] Afek, I., Ambar, O. & Silberberg, Y. High-noon states by mixing quantum and classical light. Science **328**, 879–881 (2010).

[7] Chen, G. et al. Heisenberg-scaling measurement of the single-photon kerr non-linearity using mixed states. Nature communications **9**, 1–6 (2018).

[8] Chen, G. et al. Achieving heisenberg-scaling precision with projective measurement on single photons. Physical review letters **121**, 060506 (2018).

[9] Anisimov, P. M. et al. Quantum metrology with two-mode squeezed vacuum: Parity detection beats the heisenberg limit. Physical review letters **104**, 103602 (2010).

[10] Beltrán, J. & Luis, A. Breaking the heisenberg limit with inefficient detectors. Physical review A **72**, 045801 (2005).

[11] Boixo, S., Flammia, S. T., Caves, C. M. & Geremia, J. M. Generalized limits for single-parameter quantum estimation. Physical Review Letters **98**, 090401 (2007).

[12] Roy, S. & Braunstein, S. L. Exponentially enhanced quantum metrology. Physical Review Letters **100**, 220501 (2008).

[13] Choi, S. & Sundaram, B. Bose-einstein condensate as a nonlinear ramsey interferometer operating beyond the heisenberg limit. Physical Review A **77**, 053613 (2008).

[14] Zwierz, M., Pérez-Delgado, C. A. & Kok, P. General optimality of the heisenberg limit for quantum metrology. Physical Review Letters **105**, 180402 (2010).

[15] Napolitano, M. et al. Interaction-based quantum metrology showing scaling beyond the heisenberg limit. Nature **471**, 486–489 (2011).

[16] Yang, Y. Memory effects in quantum metrology. Physical Review Letters **123**, 110501 (2019).

[17] Zhao, X., Yang, Y. & Chiribella, G. Quantum metrology with indefinite causal order. Physical Review Letters **124**, 190503 (2020).

[18] Chiribella, G., D'Ariano, G., Perinotti, P. & Valiron, B. Beyond quantum computers. arXiv preprint arXiv:0912.0195 (2009).

[19] Chiribella, G., D'Ariano, G. M., Perinotti, P. & Valiron, B. Quantum computations without definite causal structure. Physical Review A **88**, 022318 (2013).

[20] Hardy, L. Towards quantum gravity: a framework for probabilistic theories with non-fixed causal structure. J. Phys. A **40**, 3081 (2007).

[21] Oreshkov, O., Costa, F. & Brukner, Č. Quantum correlations with no causal order. Nature communications **3**, 1–8 (2012).

[22] Chiribella, G. Perfect discrimination of no-signalling channels via quantum superposition of causal structures. Phys. Rev. A **86**, 040301(R) (2012).

[23] Araújo, M., Costa, F. & Brukner, Č. Computational advantage from quantum-controlled ordering of gates. Physical review letters **113**, 250402 (2014).

[24] Guérin, P. A., Feix, A., Araújo, M. & Brukner, Č. Exponential communication complexity advantage from quantum superposition of the direction of communication. Physical review letters **117**, 100502 (2016).

[25] Ebler, D., Salek, S. & Chiribella, G. Enhanced communication with the assistance of indefinite causal order. Phys. Rev. Lett. **120**, 120502 (2018).

[26] Felce, D. & Vedral, V. Quantum refrigeration with indefinite causal order. Physical review letters **125**, 070603 (2020).

[27] Frey, M. Indefinite causal order aids quantum depolarizing channel identification. Quantum Information Processing **18**, 1–20 (2019).

[28] Mukhopadhyay, C., Gupta, M. K. & Pati, A. K. Superposition of causal order as a metrological resource for quantum thermometry. arXiv preprint arXiv:1812.07508 (2018).

[29] Chapeau-Blondeau, F. Noisy quantum metrology with the assistance of indefinite causal order. Physical Review A **103**, 032615 (2021).

[30] Procopio, L. M. et al. Experimental superposition of orders of quantum gates. Nature communications **6**, 1–6 (2015).

[31] Rubino, G. et al. Experimental verification of an indefinite causal order. Science advances **3**, e1602589 (2017).

[32] Goswami, K. et al. Indefinite causal order in a quantum switch. Physical review letters **121**, 090503 (2018).

[33] Wei, K. et al. Experimental quantum switching for exponentially superior quantum communication complexity. Physical review letters **122**, 120504 (2019).

[34] Goswami, K., Cao, Y., Paz-Silva, G., Romero, J. & White, A. Increasing communication capacity via superposition of order. Physical Review Research **2**, 033292 (2020).

[35] Taddei, M. M. et al. Computational advantage from the quantum superposition of multiple temporal orders of photonic gates. PRX Quantum **2**, 010320 (2021).

[36] Guo, Y. et al. Experimental transmission of quantum information using a superposition of causal orders. Physical review letters **124**, 030502 (2020).

[37] Aguilar, G., Piera, R., Saldanha, P., de Matos Filho, R. & Walborn, S. Robust interferometric sensing using two-photon interference. Physical Review Applied **14**, 024028 (2020).

[38] Garay, L. J. Quantum gravity and minimum length. International Journal of Modern Physics A **10**, 145–165 (1995).

[39] Szabo, R. J. Quantum field theory on noncommutative spaces. Physics Reports **378**, 207–299 (2003).

[40] Pikovski, I., Vanner, M. R., Aspelmeyer, M., Kim, M. & Brukner, Č. Probing planck-scale physics with quantum optics. Nature Physics **8**, 393–397 (2012).

[41] Kempf, A., Mangano, G. & Mann, R. B. Hilbert space representation of the minimal length uncertainty relation. Physical Review D **52**, 1108 (1995).

Acknowledgments . This work was supported by the National Key Research and Development Program of China (Nos. 2016YFA0302700, 2017YFA0304100), National Natural Science Foundation of China (Grant Nos. 11874344, 61835004, 61327901, 11774335, 91536219, 11821404), Key Research Program of Frontier Sciences, CAS (No. QYZDY-SSW-SLH003), Anhui Initiative in Quantum Information Technologies (AHY020100, AHY060300), the Fundamental Research Funds for the Central Universities (Grant No. WK2030020019, WK2470000026), Science Foundation of the CAS (No. ZDRW-XH-2019-1), the Hong Kong Research Grant Council through grant 17300918 and though the Senior Research Fellowship Scheme SRFS2021-7S02, the Croucher Foundation, and the John Templeton Foundation through grant 61466, The Quantum Information Structure of Spacetime (qiss.fr). Research at the Perimeter Institute is supported by the Government of Canada through the Department of Innovation, Science and Economic Development Canada and by the Province of Ontario through the Ministry of Research, Innovation and Science. The opinions expressed

in this publication are those of the authors and do not necessarily reflect the views of the John Templeton Foundation.

Competing interests: The authors declare no competing financial interests.

Author Contributions Peng Yin, Xiaobin Zhao, Yuxiang Yang and Giulio Chiribella proposed the framework of the theory and made the calculations. Peng Yin, Wen-Hao Zhang, Gong-Chu Li and Geng Chen planned and designed the experiment. Peng Yin and Geng Chen carried out the experiment assisted by Bi-Heng Liu, Jinshi Xu, Yongjian Han and Yu Guo. Peng Yin, Geng Chen, Xiaobin Zhao Yuxiang Yang and Giulio Chiribella analyzed the experimental results and wrote the manuscript. Guangcan Guo, Chuanfeng Li and Giulio Chiribella supervised the project. All authors discussed the experimental procedures and results.

Supplementary Files

This is a list of supplementary files associated with this preprint. Click to download.

- SM.pdf